ERAU-PHY-0201

The Driven Pendulum at Any Drive Angle

Gordon J. VanDalen*

Department of Physics, University of California, Riverside, CA 92521 and

Department of Physics, Embry-Riddle Aeronautical University, Prescott, AZ 86301

(Dated: January 28, 2003)

Abstract

The driven inverted pendulum undergoes stable oscillations if the drive amplitude and frequency are large enough. This classroom demonstration is best used in junior or graduate level Classical Mechanics courses. This paper reintroduces the equation of motion of the driven pendulum, generalizing to arbitrary driving angle. The pendulum will oscillate about a stable angle, other than straight down, if the drive amplitude and frequency are large enough for a given drive angle. We will explore what is meant by *"large enough."* Emphasis is given to parameters associated with a simply made demonstration apparatus.

I. INTRODUCTION

The general theory of the driven inverted pendulum is given in Landau and Lifshitz[1] and other advanced mechanics texts, and has been reviewed in this journal, starting with Refs. 2,3, and recently in Ref. 4. (See Ref. 4 for further citations.) An inverted pendulum demonstration was described in Ref. 5.

The UC Riverside demonstration inverted pendulum, number M17Q in the Department of Physics demonstration collection[6], is a 25cm ($L = 0.25$m) long rod mounted on a saber saw with a stroke ($2A$) of one inch, so the drive amplitude is $A = 0.0127$m. The demonstration is designed to be clamped to a table top as shown in Fig. 1, but becomes more interesting when hand held. (This is essentially the demonstration suggested in Ref. 5.) We will examine the stability of this system as a function of the angular frequency, the amplitude of the driving saber saw, and the *angle of the driving saw from the vertical.*

This type of demonstration is best used in junior level Classical Mechanics when introducing Lagrange's Equations to find the equations of motion. Examples of driving the support of a simple pendulum harmonically either in a vertical or horizontal plane can be introduced, but only to set up the equation of motion[7,8]. The actual solution for the motion can be further investigated using a computer simulation or solution by the more inquisitive students. The same apparatus can be used in an advanced graduate course in Classical Mechanics where the harmonically driven pendulum is used as an example in presenting Lagrange's equations, and as a source of exercises. The Landau and Lifshitz[1] section on "Motion in a rapidly oscillation field" uses vertically and horizontally driven pendulums as problems, and introduces the technique we use to solve for arbitrary drive angles in sections III and V.

This demonstration apparatus can at best impress, and at worse confuse lower division students, but will never be understood at that level. It does provide an excellent example of how lecture demonstrations could and should be used in advanced classes. Although I had seen the demonstration and played with it during many years of teaching the freshman sequence, it wasn't until I taught junior Classical Mechanics that I could find a way to show the device to illustrate an approachable problem.

It was after showing the inverted pendulum, clamped to a table top, that I came upon the subject of this paper. While holding the saw in my hand, with the power still on, I lowered the saw and observed the peculiar behavior of the pendulum as it found new stable

angles of oscillation as the drive angle changed. Tipping the plane of the pendulum's motion is simply equivalent to lowering the effective value of g, but changing the driving angle in the plane of the pendulum's motion introduces the new and interesting problem addressed here.

II. THE EQUATION OF MOTION OF THE PENDULUM DRIVEN AT ANY ANGLE

The dynamics of driven inverted pendulum near $\theta = 180°$ are described in Refs. 1,2,3, etc. Here we generalize the problem to arbitrary driving angles.

The geometry of the problem is illustrated in Fig. 2. A thin rod pendulum of length L is driven at its end (pivot) by a displacement with amplitude A, angular frequency ω, at an angle of $\theta_{\rm d}$ from vertical downward. The angle of the thin rod is measured by the generalized coordinate θ also measured from the vertical downward.

The angle of the rod θ could have been measured from the driving direction, $\theta_{\rm d}$. However, only for two values of $\theta_{\rm d}$ (0 and π) will the equilibrium angle of the pendulum be $\theta_{\rm d}$. For *any* value $\theta_{\rm d}$ there is a stable point for small ω and A at $\theta = 0$. So we choose to measure the pendulum angle θ from the vertical downward.

The kinetic energy and potential energy of the rod can be written in terms of one generalized coordinate θ. The energies are separated into the motion of the center of mass plus rotation about the center of mass. We first need the Cartesian coordinates of the center-of-mass expressed in terms of the generalized coordinate θ.

$$\begin{aligned} x_{\rm cm} &= +\frac{L}{2}\sin\theta + A\sin\theta_{\rm d}\cos\omega t \\ y_{\rm cm} &= -\frac{L}{2}\cos\theta - A\cos\theta_{\rm d}\cos\omega t \end{aligned} \tag{1}$$

From this we get the velocity components of the center of mass.

$$\begin{aligned} \dot{x}_{\rm cm} &= +\frac{L}{2}\dot{\theta}\ \cos\theta - A\omega\sin\theta_{\rm d}\sin\omega t \\ \dot{y}_{\rm cm} &= +\frac{L}{2}\dot{\theta}\ \sin\theta + A\omega\cos\theta_{\rm d}\sin\omega t \end{aligned} \tag{2}$$

Then we can express the kinetic energy and potential energy in terms of the generalized coordinate θ.

$$T = \frac{1}{2}m\left(\dot{x}_{\rm cm}^2 + \dot{y}_{\rm cm}^2\right) + \frac{1}{2}I_{\rm cm}\dot{\theta}^2$$

Plugging in Cartesian coordinates and velocities from Eqs. (1) and (2), we get the kinetic energy.

$$T = \frac{1}{2}m\left[\left(\frac{L}{2}\dot{\theta}\,\cos\theta - A\omega\sin\theta_{\rm d}\sin\omega t\right)^2 + \left(\frac{L}{2}\dot{\theta}\,\sin\theta + A\omega\cos\theta_{\rm d}\sin\omega t\right)^2\right] + \frac{1}{2}\left(\frac{mL^2}{12}\right)\dot{\theta}^2$$

$$T = \frac{1}{2}\left[\frac{mL^2}{3}\,\dot{\theta}^2 + mLA\omega\dot{\theta}\,(\sin\theta\cos\theta_{\rm d} - \cos\theta\sin\theta_{\rm d})\,\sin\omega t + mA^2\omega^2\sin^2\omega t\right] \tag{3}$$

We recognize the first term as rotation about the moving support at the end of the pendulum with a moment of inertia of $mL^2/3$ about that end.

Potential energy only depends on $y_{\rm cm}$ from Eq. (1).

$$V = mgy_{\rm cm} = -\frac{mgL}{2}\cos\theta - mgA\cos\theta_{\rm d}\cos\omega t \tag{4}$$

The Lagrangian is $L = T - V$, using Eqs. (3) and (4).

$$L = \frac{1}{2}\left[\frac{mL^2}{3}\,\dot{\theta}^2 + mLA\omega\dot{\theta}\,\left(\sin\theta\cos\theta_{\rm d} - \cos\theta\sin\theta_{\rm d}\right)\,\sin\omega t + mA^2\omega^2\sin^2\omega t\right] + mg\left(\frac{L}{2}\cos\theta + A\cos\theta_{\rm d}\right.$$

$$L = \frac{1}{2}\left[\frac{mL^2}{3}\,\dot{\theta}^2 + mLA\omega\dot{\theta}\,\sin\left(\theta - \theta_{\rm d}\right)\,\sin\omega t + mA^2\omega^2\sin^2\omega t\right] + mg\left(\frac{L}{2}\cos\theta + A\cos\theta_{\rm d}\right.$$

For Lagrange's equation we need two partial derivatives.

$$\frac{\partial L}{\partial\dot{\theta}} = \frac{mL^2}{3}\,\dot{\theta} + \frac{1}{2}mLA\omega\sin\left(\theta - \theta_{\rm d}\right)\,\sin\omega t \qquad \frac{\partial L}{\partial\theta} = \frac{1}{2}mLA\omega\dot{\theta}\,\cos\left(\theta - \theta_{\rm d}\right)\,\sin\omega t - \frac{mgL}{2}\sin\theta \tag{6}$$

Then the equation of motion is found from Lagrange's equation for our single generalized coordinate θ.

$$\frac{d}{dt}\left(\frac{\partial L}{\partial\dot{\theta}}\right) - \frac{\partial L}{\partial\theta} = 0 \tag{7}$$

Next we plug in partial derivatives from Eq. (6).

$$\frac{d}{dt}\left[\frac{mL^2}{3}\,\dot{\theta} + \frac{1}{2}mLA\omega\sin\left(\theta - \theta_{\rm d}\right)\,\sin\omega t\right] - \left[\frac{1}{2}mLA\omega\dot{\theta}\,\cos\left(\theta - \theta_{\rm d}\right)\,\sin\omega t - \frac{mgL}{2}\sin\theta\right] = 0$$

$$\frac{mL^2}{3}\,\ddot{\theta} + \frac{1}{2}mLA\omega\dot{\theta}\,\cos\left(\theta - \theta_{\rm d}\right)\sin\omega t + \frac{1}{2}mLA\omega^2\sin\left(\theta - \theta_{\rm d}\right)\cos\omega t - \frac{1}{2}mLA\omega\dot{\theta}\,\cos\left(\theta - \theta_{\rm d}\right)\sin\omega t + \frac{mgL}{2}$$

Two terms cancel (second and fourth), simplifying the last expression.

$$\frac{mL^2}{3}\,\ddot{\theta} + \frac{mLA\omega^2}{2}\sin\left(\theta-\theta_{\rm d}\right)\,\cos\omega t + \frac{mgL}{2}\sin\theta = 0$$

Rearranging we get the equation of motion for the *Pendulum Driven at Any Angle.*

$$\ddot{\theta} + \frac{3A\omega^2}{2L}\,\sin\left(\theta-\theta_{\rm d}\right)\,\cos\omega t + \frac{3g}{2L}\,\sin\theta = 0 \tag{8}$$

Note that if $\theta_{\rm d} = 180°$, we get the *Driven Inverted Pendulum* which has previously been discussed[1,2,3,4]. This special case is revisited briefly in section IV B and appendix A.

III. EFFECTIVE POTENTIAL

Next we introduce an *effective potential* to help us understand the physical origin of the stability of the inverted pendulum, and to parameterize the condition for stability at any driving angle.

Landau and Lifshitz[1] separate the motion of the horizontally or vertically driven pendulum into two parts: (a) a *fast* component $\xi(t)$ at the drive angular frequency ω, and (b) a *slow* component $\phi(t)$ which describes the slower overall swinging of the driven pendulum.

$$\theta(t) = \phi(t) + \xi(t) \tag{9}$$

The angle ϕ is defined as zero downward, as was θ, while ξ is the difference between θ and ϕ. In what follows we assume that the average of $\xi(t)$ (denoted $\overline{\xi}$) is zero, and that $\xi(t)$ is small compared to the slow motion $\phi(t)$.

The equation of motion for a pendulum driven at *any angle* (8) can be rearranged.

$$\ddot{\theta} = -\frac{3g}{2L}\sin\theta - \frac{3A\omega^2}{2L}\sin\left(\theta-\theta_{\rm d}\right)\cos\omega t = F(\theta) + f(\theta,t) \tag{10}$$

We have separated the angular acceleration into a time dependent driving part $f(\theta,t)$ oscillating at the driving angular frequency ω, and a time independent part $F(\theta)$ corresponding to gravity. Eq. (10) can be written in an expansion in ξ for small values of $\xi(t)$.

$$\ddot{\phi} + \ddot{\xi} \simeq F(\phi) + \frac{dF}{d\theta}(\phi)\cdot\xi + f(\phi,t) + \frac{df}{d\theta}(\phi,t)\cdot\xi$$

Keeping only the largest rapidly varying parts on each side of this equation gives

$$\ddot{\xi} \simeq f(\phi,t) = -\frac{3A\omega^2}{2L}\,\sin\left(\phi-\theta_{\rm d}\right)\,\cos\omega t \tag{11}$$

(Note that $\ddot{\xi}$ is ω^2 larger than $\xi(t)$, so the terms in ξ may safely be ignored. Also both the $\ddot{\phi}$ on the left and $F(\theta)$ on the right do not oscillate at the driving angular frequency ω.)

Eq. 11 may be integrated twice, taking the slow motion ϕ as constant on the time scale $1/\omega$.

$$\xi(t) \simeq +\frac{3A}{2L}\ \sin(\phi - \theta_{\rm d})\ \cos\omega t \tag{12}$$

Averaging Eq. (10) over the *fast* component of the motion at angular frequency ω gives the equation of motion for the slow swinging of the pendulum.

$$\ddot{\phi} + \overline{\ddot{\xi}} \simeq F(\phi) + \frac{dF}{d\theta}(\phi)\cdot\overline{\xi} + \overline{f(\phi,t)} + \overline{\frac{df}{d\theta}(\phi,t)\cdot\xi}$$

The rapidly oscillating terms $\ddot{\xi}$, ξ and $f(\phi,t)$ average to zero.

$$\ddot{\phi} \simeq F(\phi) + \overline{\frac{df}{d\theta}(\phi,t)\cdot\xi}$$

We can then plug in for $F(\phi)$, $\frac{df}{dt}$ from Eq. (10) and for $\xi(t)$ from Eq. (12).

$$\ddot{\phi} \simeq -\frac{3g}{2L}\ \sin\phi + \overline{\left[-\frac{3A\omega^2}{2L}\ \cos(\phi-\theta_{\rm d})\ \cos\omega t\right]\ \left[\frac{3A}{2L}\ \sin(\phi-\theta_{\rm d})\ \cos\omega t\right]}$$

Only the $\cos\omega t$ terms vary rapidly, and so average on the longer time scale of ϕ motion.

$$\ddot{\phi} \simeq -\frac{3g}{2L}\ \sin\phi - \frac{9A^2\omega^2}{4L^2}\ \cos(\phi-\theta_{\rm d})\ \sin(\phi-\theta_{\rm d})\ \overline{\cos^2\omega t}$$

$$\ddot{\phi} \simeq -\frac{3g}{2L}\ \sin\phi - \frac{9A^2\omega^2}{8L^2}\ \cos(\phi-\theta_{\rm d})\ \sin(\phi-\theta_{\rm d}) \tag{13}$$

Eq. (13) describes the slow swinging motion of the driven pendulum. The effective torque is the acceleration $\ddot{\phi}$ about one end of the rod multiplied by the moment of inertia about the end of the rod.

$$\tau_{\rm eff}(\phi) = \frac{mL^2}{3}\ddot{\phi} \simeq -\frac{mgL}{2}\ \left[\sin\phi + \frac{3A^2\omega^2}{4gL}\ \cos(\phi-\theta_{\rm d})\ \sin(\phi-\theta_{\rm d})\right] \tag{14}$$

This torque can be derived from an effective potential energy, $V_{\rm eff}(\phi)$.

$$V_{\rm eff}(\phi) = -\frac{mgL}{2}\ \left(\cos\phi + \frac{3A^2\omega^2}{16gL}\ \left[\cos^2(\phi-\theta_{\rm d}) - \sin^2(\phi-\theta_{\rm d})\right]\right) \tag{15}$$

The effective torque and effective potential energy are simply related.

$$\tau_{\rm eff}(\phi) = -\frac{dV_{\rm eff}}{d\phi}$$

Combining the trigonometric functions in Eqs. (14) and (15) simplify the expressions for the effective torque and effective potential.

$$\tau_{\text{eff}}(\phi) = -\frac{mgL}{2}\left(\sin\phi + \frac{3A^2\omega^2}{8gL}\ \sin\left[2\left(\phi-\theta_{\text{d}}\right)\right]\right)$$
$$V_{\text{eff}}(\phi) = -\frac{mgL}{2}\ \left(\cos\phi + \frac{3A^2\omega^2}{16gL}\ \cos\left[2\left(\phi-\theta_{\text{d}}\right)\right]\right) \tag{16}$$

Defining the dimensionless critical parameter R, and the critical angular frequency ω_{c}.

$$R = \frac{3A^2\omega^2}{4gL} = \frac{\omega^2}{\omega_{\text{c}}^2} \qquad\qquad \omega_{\text{c}} = \sqrt{\frac{4gL}{3A^2}} \tag{17}$$

We can rewrite the effective potential from Eq. 16.

$$V_{\text{eff}}(\phi) = -\frac{mgL}{2}\ \left(\cos\phi + \frac{R}{4}\ \cos\left[2\left(\phi-\theta_{\text{d}}\right)\right]\right) \tag{18}$$

The first term in the potential energy is simply gravity acting on the center of mass of the pendulum. The second term comes from the *dynamics* of the forced motion, and representing the average kinetic energy of the rapidly driven oscillation of the pendulum about its center of mass. As the pendulum deviates from the drive angle (θ_{d}) the angular kinetic energy of the pendulum about its center of mass increases.

The kinetic energy associated with the driving angular frequency, treated as an effective potential energy, stabilizes the slow motion of the inverted pendulum. Fig. 3 shows the effective potential as a function of ϕ for a driven inverted pendulum with $R = 1.75$, as it is for UC Riverside demonstration M17Q. In Fig. 3 we see the gravitational potential minimum at $\phi = 0$ and also the *dynamic* potential minimum at $\phi = 180°$. If the drive amplitude or angular frequency become too small ($R \leq 1$), then the stable equilibrium at $\phi = 180°$ disappears. (Note that the local *maximum* near 125 degrees limits the amplitude of slow oscillation of this particular case of a driven inverted pendulum.)

The same physical interpretation of the driven wobble of the pendulum as a stabilizing effective torque is seen in Eq. (14) which includes a stabilizing part depending on ω^2 which originated in the kinetic energy of rotation at the driving angular frequency ω. (This is basically the same as the way in which centrifugal force in orbital motion originates from rotational kinetic energy about the center of mass when reducing to a radial equation of motion.)

IV. SPECIAL CASES OF THE DRIVE ANGLE

Let us look at three special cases before moving on to general values of $\theta_{\rm d}$. These three examples will provide some guidance in interpreting the result for an arbitrary driving angle $\theta_{\rm d}$.

A. Drive angle zero degrees

If $\theta_{\rm d} = 0$, we get the equation of motion for the slow oscillation $\phi(t)$ from Eq. (13), using $\theta_{\rm d} = 0$.

$$\ddot{\phi} + \left(\frac{3g}{2L} + \frac{9A^2\omega^2}{8L^2} \cos\phi \right) \sin\phi = 0$$

For small angles $\phi \sim 0$ we can take $\cos\phi \simeq 1$ and also $\sin\phi \simeq \phi$.

$$\ddot{\phi} + \frac{3g}{2L} \left(1 + \frac{3A^2\omega^2}{4gL} \right) \phi = \ddot{\phi} + \omega_{\rm p}^2 \, \phi \simeq 0 \tag{19}$$

The pendulum oscillates slowly about $\phi = 0$ with an angular frequency $\omega_{\rm p}$ which is the square-root of the coefficient of the term in $\phi(t)$.

$$\omega_{\rm p} = \omega_0 \sqrt{1 + \frac{3A^2\omega^2}{4gL}} = \omega_0 \sqrt{1 + \frac{\omega^2}{\omega_{\rm c}^2}} = \omega_0 \sqrt{1+R}$$

We have used $\omega_0 = \sqrt{3g/2L}$ which is the angular frequency of the undriven pendulum. Driving the pendulum increases its frequency (decreases its period).

The UC Riverside demonstration driven pendulum has $R = 1.75$ and $f_0 = \omega_0/2\pi = 1.2$Hz, so has a frequency of $f_{\rm p} = 1.66 f_0 = 2.0$Hz when driven vertical with the rod hanging down.

B. Drive angle 180 degrees

When $\theta_{\rm d} = 180^\circ = \pi$, let $\delta = \phi - \pi$ so we get the *Driven Inverted Pendulum* from Eq. (13).

$$\ddot{\delta} + \left(\frac{9A^2\omega^2}{8L^2} \cos\delta - \frac{3g}{2L} \right) \sin\delta = 0 \tag{20}$$

Small angles δ allow the approximations used above.

$$\ddot{\delta} + \frac{3g}{2L} \left(\frac{3A^2\omega^2}{4gL} - 1 \right) \delta = \ddot{\delta} + \omega_{\rm p}^2 \, \delta \simeq 0 \tag{21}$$

which gives small oscillations with an angular frequency

$$\omega_{\rm p} = \omega_0 \sqrt{\frac{3A^2\omega^2}{4gL} - 1} = \omega_0 \sqrt{\frac{\omega^2}{\omega_{\rm c}^2} - 1} = \omega_0 \sqrt{R-1}$$

We get stable small oscillations only if $R > 1$ or equivalently $\omega > \omega_{\rm c}$. The UC Riverside driven inverted pendulum has $f_{\rm p} = 0.86 f_0 = 1$Hz, or about half the frequency when driven hanging down ($\theta_{\rm d} = 0$).

Appendix A reviews the traditional treatment of the inverted pendulum starting with Eq. (8). The solution of the linearized equation of motion for $\theta_{\rm d} = 180°$ gives the *Mathieu* functions[9] with well known properties. Only for a limited range of drive amplitude and angular frequency do we get stable oscillations of the driven inverted pendulum. The range of stability is usually displayed in terms of *Mathieu parameters* (see Fig. 15 in Appendix A).

Fig. 4 displays the regions of stability of the *Mathieu* functions plotted in terms of pendulum drive parameters A and ω for the UC Riverside demonstration with $L = 0.25$m. The lower smooth curve in Fig. 4 is approximately $A\omega = 1.81$m/s. The point is at approximately the operating point of the UC Riverside (30Hz,0.5inch). Note that we should also avoid *large* driving amplitudes ($A > 0.08$m) for a 25cm rod. The effective potential technique of Landau and Lifshitz[1] is also not valid for large drive parameters, so does not address an upper stability limit. A numerical solution of the equation of motion (8) is needed to explore shorter bars (or large driving amplitudes) together with slow oscillation angular amplitudes larger than the linear approximation supports.

Full numerical simulations of the equation of motion (8), including *ad hoc* frictional damping, for both $\theta_{\rm d} = 0$ and $\theta_{\rm d} = 180°$ are shown in Fig. 5. Appendix B presents the technique used to generate these simulations, and others shown below.

Fig. 6 shows for very short rods that interesting, non-oscillatory behavior results. The UC Riverside demonstration appears to be unstable in numerical solutions for any rod length less than 4cm. This suggests other studies of overdriven parametric systems which can be simply realized with a driven mechanical pendulum. Previous studies[10,11] could easily be extended to arbitrary drive angles using the analysis in section V below.

C. Drive angle 90 degrees

Using a drive angle $\theta_{\rm d} = 90^\circ = \pi/2$, the equation of motion for slow oscillation Eq. (13) reduces to a simple form.

$$\ddot{\phi} + \left(\frac{3g}{2L} - \frac{9A^2\omega^2}{8L^2} \cos\phi \right) \sin\phi = 0 \tag{22}$$

For small angles ϕ ($\cos\phi \sim 1$ and $\sin\phi \sim \phi$) we get

$$\ddot{\phi} + \frac{3g}{2L}(1 - R)\ \phi \simeq 0$$

This equation gives small oscillations near $\phi = 0$ only if $\omega < \omega_{\rm c}$ or $R < 1$.

However, if $\omega > \omega_{\rm c}$ ($R > 1$), the term in parentheses is negative, and there *cannot be stable oscillation near* $\phi = 0$. To find the new location for the stable equilibrium angle (ϕ_0), take $\phi = \delta + \phi_0$ in Eq. (22).

$$\ddot{\delta} + \frac{3g}{2L}\left[1 - R\ \cos\left(\delta + \phi_0\right)\right]\ \sin\left(\delta + \phi_0\right) = 0 \tag{23}$$

We get the equilibrium angle ϕ_0 by taking $\delta = 0$ and $\ddot{\delta} = 0$.

$$\left[1 - R\ \cos\phi_0\right]\ \sin\phi_0 = 0 \tag{24}$$

The solution $\phi_0 = 0$ which we have already seen, is only stable if $\omega < \omega_{\rm c}$ ($R < 1$). Equation (24) also has a second solution valid for $R > 1$.

$$1 - R\ \cos\phi_0 = 0$$

The equilibrium angle ϕ_0 is nonzero and finite for $R > 1$.

$$\phi_0 = \cos^{-1}\frac{1}{R} \tag{25}$$

Observe that $0 < \phi_0 \leq \pi/2$ for $R > 1$ (or $\omega > \omega_{\rm c}$).

Near equilibrium this second solution should reduce Eq. (23) to an approximate harmonic oscillator.

$$\ddot{\delta} + \omega_{\rm p}^2\ \delta \simeq 0$$

This gives a *stable* equilibrium only if the coefficient of δ is positive.

$$\frac{d}{d\delta}\left\{\left[1 - R\ \cos\left(\delta + \phi_0\right)\right]\ \sin\left(\delta + \phi_0\right)\right\}_{\delta=0} > 0$$

$$[1 - R\ \cos\phi_0]\ \cos\phi_0 + R\ \sin^2\phi_0 > 0 \tag{26}$$

The requirement that we have equilibrium at ϕ_0 in Eq. (24) makes the first term in Eq. (26) zero. Then

$$R\ \sin^2\phi_0 > 0$$

which is true for all $0 < \phi_0 \leq \pi/2$ ($\omega > \omega_c$ or $R > 1$).

The *effective torque* here came from averaging small oscillations at the driving angular frequency ω to get Eq. (14). Using $\theta_d = 90°$ in Eq. (14) gives the effective torque for $\theta_d = 90°$.

$$\tau_{\rm eff}(\phi) = -\frac{mgL}{2}\left(1 - \frac{3A^2\omega^2}{4gL}\ \cos\phi\right)\ \sin\phi$$

Setting the torque equal to zero at $\phi = \phi_0$ gives the same equilibrium condition as Eq. (25). Requiring a positive curvature of the potential is equivalent to Eq. (26).

Fig. 7(a) shows the effective potential for $R = 1.75$ with a stable minimum at $\phi_0 = 55°$. The effective potential for $R = 0.75 < 1$ is shown in Fig. 7(b), where the only minimum in the potential is at $\phi_0 = 0$.

The full numerical simulation matches the simplified model giving stable oscillation near $\theta = \phi_0 \simeq 55°$ in Fig. 8(a) for $R = 1.75$. Taking the same system with a drive angular frequency of 123rad/s (corresponding to $R = 0.75 < 1$) only gives stable oscillation about zero degrees when the drive angle is $\theta_d = 90°$ in Fig. 8(b).

The horizontally driven pendulum ($\theta_d = 90°$) is

- stable hanging down ($\phi_0 = 0$) for $R < 1$, and
- stable near $\phi_0 = \cos^{-1}(1/R)$ for $R > 1$.

Now let us look at other drive angles.

V. THE DRIVEN PENDULUM AT OTHER ANGLES

Starting with the equation of motion (13) for a general drive angle θ_d.

$$\ddot{\phi} + \frac{3g}{2L}\ [\sin\phi + R\ \cos(\phi - \theta_d)\ \sin(\phi - \theta_d)] \simeq 0$$

Equilibrium occurs when $\phi = \phi_0$ with $\ddot{\phi} = 0$.

$$\sin\phi_0 + R\ \cos(\phi_0 - \theta_d)\ \sin(\phi_0 - \theta_d) = 0 \tag{27}$$

Combining the product of trigonometric functions gives an equivalent result.

$$\sin\phi_0 + \frac{R}{2}\ \sin\left[2\left(\phi_0 - \theta_\mathrm{d}\right)\right] = 0 \tag{28}$$

The equilibrium is *stable,* as we have seen above, if

$$\frac{d}{d\phi}\left[\sin\phi + R\ \cos\left(\phi - \theta_\mathrm{d}\right)\ \sin\left(\phi - \theta_\mathrm{d}\right)\right]_{\phi=\phi_0} > 0$$

which gives

$$\cos\phi_0 + R\ \left[\cos^2\left(\phi_0 - \theta_\mathrm{d}\right) - \sin^2\left(\phi_0 - \theta_\mathrm{d}\right)\right] > 0.$$

The trigonometric functions can be simplified.

$$\cos\phi_0 + R\ \cos\left[2\left(\phi_0 - \theta_\mathrm{d}\right)\right] > 0 \tag{29}$$

Small oscillations about the equilibrium angle ϕ_0 have angular frequency ω_p.

$$\omega_\mathrm{p} = \omega_0\ \sqrt{\cos\phi_0 + R\ \cos\left[2\left(\phi_0 - \theta_\mathrm{d}\right)\right]}$$

The condition for equilibrium in Eq. (28) can be easily solved for θ_d as a function of ϕ_0, which can be a multivalued function. However, we wish to know the stable angle of oscillation ϕ_0 as a function of the drive angle θ_d.

Simply finding the solutions of Eq. (28) is not sufficient. The zeroes must correspond to real angles and to *stable* equilibriums as defined by Eq. 29. Applying all necessary tests leads us to use "Procedural Programming" in `Mathematica` in the form of the `Block` structure. (See Appendix C.)

Fig. 9(a) shows that the UC Riverside inverted pendulum demonstration has a range of drive angles for which there are no (nearby) stable equilibrium angles. For all values of $R \geq 2$ there is a stable equilibrium ϕ_0 for all drive angles θ_d. The critical case $R = 2$ is shown in Fig. 9(b). For values of $R > 2$ the curve representing $\phi_0(\theta_\mathrm{d})$ becomes smooth, tending to a straight line as $R \to \infty$. (But we must beware of instability appearing at larger drive parameters, equivalent to large R. There are practical limits to how large R can be to give a stable driven pendulum in a physical system.)

If we plot all solutions up to 360° in ϕ_0 (Fig. 10), we see that in the range of missing angles in Fig. 9(a) there are corresponding points which would be stable for $\theta_\mathrm{d} + 180°$. The original problem shown in Fig. 2 has this two-fold ambiguity of drive angles at θ_d and $\theta_\mathrm{d} + 180°$. In

practice our apparatus limits the motion of the rod so that we cannot observe oscillation for $|\theta_{\rm d} - \phi_0| > 90°$.

The UC Riverside demonstration M17Q with $R = 1.75$, has *no stable equilibriums* in the range $110° < \theta_{\rm d} < 160°$. Observed and calculated equilibrium angles agree within reason (see table I). This demonstration apparatus has fixed drive amplitude (A) and angular frequency (ω), so only the rod length L is adjustable. **Shortening** the stick on the demonstration to 20cm would give $R = 2.18$ assuring stable oscillation for any value of $\theta_{\rm d}$.

The value $R = 1$ ($\omega = \omega_{\rm c}$) defines the minimum condition for stable inverted oscillations. Fig. 11(a) show the stable angles ϕ_0 as a function of drive angle $\theta_{\rm d}$ for $R = 0.90$. Only drive angles below 90° give stable oscillations. (Note also that the stable angle for $\theta_{\rm d} = 90°$ becomes $\phi_0 = 0$ for $R \leq 1$.) Fig. 11(b) shows that for $R = 1.2$ there is a small range of $\theta_{\rm d}$'s near 180° for which stable inverted oscillation is possible, but only for small angular deviations from 180°.

Finally we graph in Fig. 12 the actual motion for R values of 0.90 and 1.20 both with $\theta_{\rm d} = 180°$ and $\theta_0 = 170°$. As expected the case of $R = 0.90 < 1$ swings down to eventual equilibrium at $\phi_0 = 0$, while for $R = 1.20 > 1$ there is a limited range of stable inverted oscillation.

VI. THE EMBRY-RIDDLE DEMONSTRATION

The desire for more degrees of freedom on a limited budget has led to the Embry-Riddle Aeronautical University driven pendulum demonstration shown in Fig. 13. A small hand-held *variable speed* Jig Saw (0 to 3200 strokes per minute) with an peak-to-peak amplitude of 0.7 inch. Converting to the units used here gives values of ω and A to be used in equations and simulations.

$$0 < \omega < 335\text{rad/s} \qquad\qquad A = 0.00889\text{m}$$

Modern saber saws offer a similar range of stroke rates, but with a peak-to-peak amplitude of 1 inch, at about 3 times the cost. The UCR demonstration saber saw has a more limited range of speed adjustment. We have made rods with lengths of approximately $L = 10$cm, 20cm and 30cm. The $L = 20$cm rod gives R as large as 3.2, well into the regime where the driven pendulum is stable at all driving angles.

The rods are made out of light wood (sections of a meter stick or yard stick) with a hole

near one end reinforced by a small metal grommet. The reinforcing is to reduce wear at the pivot. A wide jig saw blade has a small hole drilled near the end. A brass screw, washers and nuts are used to loosely fasten the rod, allowing it to swing freely[12]. The whole mechanism is light enough that the jig saw can still reach its maximum stroke rate.

The R value can be measured using Eq. (25).

$$\phi_0 = \cos^{-1}\frac{1}{R} \qquad \text{for} \qquad R > 1$$

Hold the driving saw blade horizontally and measure the angle to which the driven pendulum rises. At low driving speeds it will oscillate about the downward direction. Once $\omega > \omega_c$ the pendulum will slowly rise with increasing drive speed until a maximum angle is reached. Any angle above 60° will correspond to $R > 2$, which gives stable driven oscillations at any driving angle. We have used this method to measure the maximum R of each of our larger pendulums. The 20cm pendulum, shown in Fig. 14, has a measured maximum R of 3.2, corresponding to $\phi_0(90°) \simeq 72°$.

Fig. 14 shows the 20cm ERAU pendulum driven with $\theta_d = 135°$, having damped into a steady position near $\phi_0(135°) \simeq 118°$. The smallest pendulum as a maximum R value above 40. At lower driving rates (lower ω decreases R) it displays the behaviors expected from a driven pendulum. However, at the fastest speed of the jig saw it rotates at about one revolution per second about the driving support. Asymmetry of the pendulum determines the chirality of the motion, as flipping the pendulum over on the support screw reverses its rotation. It would appear that friction limits the rate of rotation below what one might expect from Fig. 6.

VII. CONCLUSIONS

The pendulum driven at any angle can be studied using the effective potential method of Landau and Lifshitz for rapid driving angular frequency ($\omega \gg \omega_p$). The condition for stable oscillation can be established using the effective potential Eq. (15).

Numerical simulations of the full equation of motion Eq. (8) generally confirm the results of the simplified model for high driving angular frequencies $\omega \gg \omega_p$. General behavior of the pendulum driven into small oscillations at any driving angle is summarized by the parameter

$$R = \frac{3A^2\omega^2}{4gL} = \frac{\omega^2}{\omega_c^2} \qquad \text{with} \qquad \omega_c = \sqrt{\frac{4gL}{3A^2}}$$

The pendulum will oscillate about an equilibrium angle $\phi_0(\theta_d)$ with an angular frequency ω_p.

$$\omega_p = \omega_0 \sqrt{\cos\phi_0 + R\ \cos\left[2\left(\phi_0 - \theta_d\right)\right]}$$

Here $\omega_0 = \sqrt{3g/2L}$ is the natural angular frequency of the rod as a non-driven pendulum.

The stability of the driven pendulum at any angle depends on the parameter R.

- $R \leq 1$

  no stable inverted oscillations near 180°

  stable oscillations with $\phi_0 > 0$ for all $0 < \theta_d < 90°$

  $\lim_{\theta_d \to 90°} \phi_0 = 0$

- $1 < R < 2$ stable inverted oscillations near 180°

  some range of angles between $90° < \theta_d < 180°$ will not give stable oscillations with $|\theta_d - \phi_0| < 90°$

  $\phi_0(90°) > 0$

- $R \geq 2$ stable with $|\phi_0 - \theta_d| < 90°$ for all θ_d.

All parameters of the driven pendulum are accessible over interesting ranges with simple and inexpensive apparatus: drive angle θ_d, amplitude A, bar length L, and driving angular frequency ω. Even g can be reduced by tipping the plane of oscillation. We have explored more parameter sets than reported here, and hope that others will explore and report their own variations of the driven pendulum at angles other than 0° or 180°.

Design your driven pendulum to display the range of behaviors you are interested in, and *use this demonstration (and others) in upper division and graduate mechanics classes.*

APPENDIX A: APPROXIMATE ANALYTIC SOLUTION OF THE INVERTED PENDULUM

Section IV B introduced the solution of the inverted pendulum based on the effective potential approach of Landau and Lifshitz. This system can also be easily solved by *linearizing* the equation of motion as in Ref. 3.

We can start with the general equation of motion for the driven inverted pendulum Eq. (20).

$$\ddot{\delta} + \left(\frac{3A\omega^2}{2L} \cos\omega t - \frac{3g}{2L} \right) \sin\delta \simeq 0$$

For small angles this simplified to Eq. (21).

$$\ddot{\delta} + \left(\frac{3A\omega^2}{2L} \cos\omega t - \frac{3g}{2L} \right) \delta \simeq 0$$

This has the form of *Mathieu's differential equation*[9].

$$\frac{d^2y}{dz^2} + (a - 2q\cos 2z)\, y = 0 \tag{A1}$$

Make the substitution $z = \omega t/2$ and our equation of motion can be rewritten in the Mathieu form.

$$\frac{d^2\delta}{dz^2} + \left(-\frac{6g}{L\omega^2} + \frac{6A}{L}\cos 2z \right) \delta = 0 \tag{A2}$$

where the *Mathieu parameters* are then found by comparing Eqs. (A1) and (A2).

$$q = -\frac{3A}{L} \qquad\qquad a = -\frac{6g}{L\omega^2} \tag{A3}$$

The general solutions of Mathieu's differential equation are expressed by the even and odd *Mathieu functions.* These solutions are also known to `Mathematica` as `MathieuC[a,q,z]` and `MathieuS[a,q,z]`

`Mathematica` can even recognize the solution of the Mathieu equation and can interpret a and q in terms of our parameters.

```
DSolve[y''[t] +
    ((3 A w^2/(2 L)) Cos[w t]-(3 g/(2L))) y[t]==0,y[t],t]


                          -6 g  -3 A  t w
{{y[t] -> C[1] MathieuC[----, ----, ---] +
                            2   L     2
                         L w

                                      -6 g  -3 A  t w
>                         C[2] MathieuS[----, ----, ---]}}
                                        2   L     2
                                     L w
```

For *a portion* of the parameter space in (a, q) the Mathieu functions are real and periodic, corresponding to stable equilibrium of the inverted driven pendulum. Outside of this portion of the parameter space the functions are complex and divergent, corresponding to unstable oscillation.

The region of parameter space that gives stable oscillations[9] is defined through the Mathieu parameters a and q.

$$1 - |q| - \frac{q^2}{8} + \frac{|q|^3}{128} - \frac{q^4}{1536} - \frac{11|q|^5}{36864} + \cdots = a_1(q) > a \tag{A4}$$

$$a > a_0(q) = -\frac{q^2}{2} + \frac{7q^4}{128} - \frac{29q^6}{2304} + \cdots \tag{A5}$$

For the UC Riverside demonstration pendulum we have $q = -\frac{3A}{L} = -0.1524$ so $q^2 \ll 1$. Then, to a good approximation the lower limit from Eq. (A5) simplifies to the leading term.

$$a = -\frac{6g}{L\omega^2} > -\frac{q^2}{2} = -\frac{(3A/L)^2}{2}$$

Solving for the minimum angular frequency for stable inverted driven oscillations gives a familiar result.

$$\omega > \omega_c = \sqrt{\frac{4gL}{3A^2}} = \sqrt{\frac{4(9.8\text{m/s}^2)(0.25\text{m})}{3(0.0125\text{m})^2}} = 142.3\text{rad/s}$$

Including the q^4 correction above gives $\omega_c = 142.49$rad/s. The actual apparatus does not warrant this level of precision, so we could safely devise a stable driven inverted pendulum using $A\omega > \sqrt{4gL/3}$.

Fig. 15 is commonly used to display stable regions in the Mathieu parameter space of (a, q). It is more useful for our purposes to transform into the drive parameter space of (A, ω, L). Inverting the first few terms of the Eqs. (A4) and (A5) above for $a_0(q)$ and $a_1(q)$ gives lower and upper limits in drive amplitude A as a function of drive angular frequency ω and pendulum rod length L.

$$A > A_0(\omega, L) = \frac{L}{3}\sqrt{\frac{64 - \sqrt{4096 - 3584\frac{6g}{L\omega^2}}}{14}}$$

$$A < A_1(\omega, L) = \frac{L}{3}\left(-2 + \sqrt{2}\sqrt{3 + \frac{6g}{L\omega^2}}\right)$$

```
a0[q_] := -(q^2/2) +(7 q^4/128) -(29 q^6/2304)
a1[q_] := 1 -Abs[q] -(q^2/8) +(Abs[q^3]/64) -(q^4/1536) -
                                    (11 Abs[q^5]/36864)
Plot[{a0[q],a1[q]},{q,-1,1},PlotRange->{-1,1}]
Show[%,Graphics[{PointSize[0.015],RGBColor[1,0,0],
  Point[{-0.1524,-0.00665}]}],PlotRange->{{-1,1},{-1,1}}]


A0[w_,L_]:=
   (L/3) Sqrt[(64 -Sqrt[4096 -3584(6*9.8/(L w^2))])/14]
A1[w_,L_]:=(2 L/3) (-2 +Sqrt[2] Sqrt[3 +(6*9.8/(L w^2))])
Plot[{A0[w,0.25],A1[w,0.25]},{w,1,400},
  PlotRange->{0.001,0.10},PlotStyle->{Thickness[0.008]}]
Show[%,Graphics[{PointSize[0.015],RGBColor[1,0,0],
  Point[{188,0.0127}]}],PlotRange->{{1,400},{0.001,0.1}}]
```

The first four Mathematica commands generate Fig. 15 shown in this appendix, while the last 4 lines generate Fig. 4 given in section IV B.

APPENDIX B: NUMERICAL SOLUTION OF THE GENERAL EQUATION OF MOTION

In the linear approximation, stability or instability of the equation of motion was independent of the amplitude of the motion. When we cannot safely use $\sin\theta \simeq \theta$, then we must use a numerical solution.

The general equation of motion (8) for the driven pendulum is

$$\ddot{\theta} + \frac{3A\omega^2}{2L}\,\sin\left(\theta - \theta_{\rm d}\right)\,\cos\omega t + \frac{3g}{2L}\,\sin\theta = 0$$

```
RealNumUp[A_,w_,L_,thd_,th0_] :=
     NDSolve[{th''[t]+(3 A w^2 Cos[w t] Sin[th[t]-thd]+
     3*9.8Sin[th[t]])/(2 L) == 0
     ,th[0]==th0,th'[0]==0},th,{t,0,5},MaxSteps ->50000]
RealNumUp[0.0127,188,0.25,Pi,Pi+0.1]
```

```
Plot[180*Evaluate[(th[t] /. %)]/Pi,{t,0,5}]


RealNumUp[0.0127,188,0.25,Pi,Pi-1.022]
Plot[180*Evaluate[(th[t] /. %)]/Pi,{t,0,5}]
```

Taking $\omega = 188$rad/s, the oscillation is stable for all starting angles above 121.5°, including the case shown in Fig. 16(a) with $\theta_0 = 185.7°$. Fig. 16(b) shows that the case of $\theta_0 = 121.4°$ is just barely unstable, falling to oscillation about 0°, the downward direction. Our demonstration pendulum limits the rod's motion to the range of about $\pm 110°$, and when it strikes the mechanical stop it leaps back upward, sometimes into stability.

The real demonstration has *damping* which quickly reduces oscillation to the point where the inverted pendulum remains upright at $\theta = 180°$. The following two calculations consider both constant frictional damping (torque opposing rotation) and viscous drag (proportional to angular velocity).

```
RealNumUp[A_,w_,L_,thd_,th0_] :=
     NDSolve[{th''[t]+(3 A w^2 Cos[w t] Sin[th[t]-thd]+
     3*9.8Sin[th[t]])/(2 L)==-0.5*Sign[th'[t]]
     ,th[0]==th0,th'[0]==0},th,{t,0,10},MaxSteps ->50000]
RealNumUp[0.0127,188,0.25,Pi,Pi+0.3]
Plot[180*Evaluate[th[t] /. %]/Pi,{t,0,10}]


RealNumUp[A_,w_,L_,thd_,th0_] :=
     NDSolve[{th''[t]+(3 A w^2 Cos[w t] Sin[th[t]-thd]+
     3*9.8Sin[th[t]])/(2 L)==-0.5*th'[t]
     ,th[0]==th0,th'[0]==0},th,{t,0,10},MaxSteps ->50000]
RealNumUp[0.0127,188,0.25,Pi,Pi+0.3]
Plot[180*Evaluate[th[t] /. %]/Pi,{t,0,10}]
```

The *constant friction* form gives a rapid linear decrease in oscillation amplitude, while the *viscous damping* gives the familiar under-damped oscillation with an exponentially decreasing amplitude. Our demonstration pendulums seem to be better described by *constant*

friction.

$$\ddot{\theta} + \frac{3A\omega^2}{2L}\,\sin(\theta - \theta_{\rm d})\,\cos\omega t + \frac{3g}{2L}\,\sin\theta = -\kappa\,\frac{|\dot{\theta}|}{\dot{\theta}} \qquad \text{(B1)}$$

where κ is a constant frictional torque divided by the moment of inertia. Values of κ on the order of one appear to work well for our apparatus, although adjustment is sometimes needed.

This equation of motion with constant friction (B1) can be solved for initial conditions [we choose $\theta(0) = \theta_0$ and $\dot{\theta}(0) = 0$] using `NDSolve` as shown here. Note that the drive amplitude A, the driving angular frequency ω, and the rod length L are all input in SI units, allowing simulation of a design before actually making the apparatus.

```
RealNumUp[A_,w_,L_,thd_,th0_] :=
     NDSolve[{th''[t]+(3 A w^2 Cos[w t] Sin[th[t]-thd]+
     3*9.8Sin[th[t]])/(2 L)==-5.0*Sign[th'[t]]
     ,th[0]==th0,th'[0]==0},th,{t,0,10},MaxSteps ->50000]
RealNumUp[0.0127,188,0.25,Pi/2,1.2]
Plot[180*Evaluate[(th[t] /. %)]/Pi,{t,0,10}]
```

These particular commands were used to generate Fig. 8(a).

APPENDIX C: FINDING STABLE MINIMUM NEAREST THE DRIVE ANGLE

The `Mathematica` routine `Solve` returns a list of possible solutions using inverse trigonometric functions defined in the range $-\pi < \phi_0 < \pi$. Within the same `Block` we can also add the missing analytic solution at π radians for $\theta_{\rm d} = \pi$, and shift solutions of the inverse trigonometric functions into the range $0 \le \phi \le 2\pi$.

The `Mathematica` code to obtain the stable minimum (if any) nearest to the drive angle is

```
   (* angular dependence of the potential *)
V[phi_,th0_,R_] :=  - (Cos[phi] + (R/4) Cos[2(phi-th0)])
   (* force as negative derivative of potential *)
F[phi_,th0_,R_] = - D[V[phi,th0,R],phi]
   (* potential curvature *)
```

```
Kurv[ph0_,th0_,R_] =  Re[D[D[V[ph0,th0,R],ph0],ph0] ]
   (* the condition for equilibrium *)
fun[th_,R_] := fun /. Solve[F[fun,th,R] ==0,fun]
   (* test for real value *)
test[e_] := Im[e] == 0

ph0[thd_,Rat_] :=
  Block[{th=thd*Pi/180,R=Rat,ang,angadd,len,i,Kmin},
(* get list of extrema *)
  ang = fun[th,R];
(* add sol'n at Pi if thd=Pi *)
  If[th==Pi,ang = Append[ang,Pi],{}];
(* remove complex solutions *)
  ang = Select[ang,test];
  len = Length[ang];
(* use range 0 --> 2Pi *)
  For [i=1,i<=len,i++,If[ang[[i]]<0,
                         ang[[i]]=ang[[i]]+2 Pi,{}]];
  dthmin = Pi;
  len = Length[ang];
  val = Undefined;
  For [i=1,i<=len,i++,
(* test for minima nearest drive angle *)
    If[Kurv[ang[[i]],th,R] >0 &&
    Abs[ang[[i]]-th] <= dthmin,{dthmin=Abs[ang[[i]]-th];
       val = ang[[i]]*180/Pi},{}]];
  Return[val]   ]
```

This code returns a value of $\phi_0(\theta_{\rm d}, R)$ which can be plotted with all angles in degrees.

The `ImplicitPlot` function can graph all zeroes of the force, while a simple `Plot` gives the set of stable equilibriums. The plots are then overlaid. (Note that a torque with degree arguments is defined as `Fdeg`.)

```
V[phi_,th0_,R_] :=  - (Cos[phi] + (R/4) Cos[2(phi-th0)])
Fdeg[phi_,th0_,R_] = - D[V[phi*Pi/180,th0*Pi/180,R],phi]
Needs["Graphics`ImplicitPlot`"]
ImplicitPlot[Fdeg[phi,thd,1.75]==0,{thd,0,180},
     {phi,0,180},PlotPoints->{50,50},
     PlotStyle->{{Dashing[{0.02,0.02}]}}]
Plot[ph0[thd,1.75],{thd,0,180},AspectRatio ->1,
     PlotRange->{0,180},PlotStyle->{{Thickness[0.01]}}]
Show[%,%%]
```

This code produced Fig. 9.

ACKNOWLEDGMENTS

I would like to thank Ron Ebert of UC Riverside for maintaining and documenting the many lecture demonstrations used in countless classes, and for first introducing me to the driven inverted pendulum. Thanks also to Prof. Darrel Smith and Embry-Riddle Aeronautical University for allowing me to spend a sabbatical with them, and for giving me the time to write this paper. Finally, thanks to Prof. José Wudka for pointing out the Landau and Lifshitz section on Parametric Oscillations, for sharing my amusement with these little toys, and for encouraging me to write this all down.

---

* Electronic mail: gordon.vandalen@ucr.edu; Home page: `http://physics.ucr.edu/~vandalen/`

[1] L.M. Landau and E.M. Lifshitz, "Mechanics", Pergamon (1960)

[2] F. M. Phelps, III AND J. H. Hunter, Jr., "An analytic solution of the inverted pendulum," Am. J. Phys. **33** 285-295 (1965); Am. J. Phys. **34**, 533-535 (1966).

[3] Douglas J. Ness, "Small Oscillations of a Stabilized, Inverted Pendulum," Am. J. Phys. **35**, 964 (1967)

[4] Eugene I. Butikov, "On the dynamic stabilization of an inverted pendulum," Am. J. Phys. **69**, 755-768 (2001)

[5] Herbert Jones, "A Quick Demonstration of the Inverted Pendulum," Am. J. Phys. **37**, 941 (1969)

[6] http://phyld.ucr.edu/Mechanics%20IV/M-17Q.htm

[7] Jerry B. Marion and Stephen T. Thornton, "Classical Mechanics of Particles and Systems," Fourth Edition, Saunders College Publishing (1995)

[8] Keith R. Symon, "Mechanics," Third Edition, Benjamin Cummings (1971)

[9] M. Abramowitz and I.A. Stegun, "Handbook of Mathematical Functions," Dover Publications, Inc., New York (1970)

[10] B. Duchesne, C. W. Fischer, C. G. Gray, and K. R. Jeffrey, "Chaos in the motion of an inverted pendulum: An undergraduate laboratory experiment," Am. J. Phys **59** 987 (1991)

[11] R. L. Kautz, "Chaos in a computer-animated pendulum," Am. J. Phys **61** 407 (1993)

[12] We have used #6 brass hardware (screws, washers and nuts) which is suitable to the drive system and large pendulums. To investigate *over-driven* behavior with a small pendulum a few centimeters long, small hardware should be used to reduce frictional damping.

TABLE I: Comparison of UC Riverside demonstration with stable angles calculated here.

θ_d	ϕ_0 calculation in FIG: 9(a)	ϕ_0 for Demo M17Q
0	0	~ 0
30°	19°	$\sim 15°$
60°	38°	$\sim 35°$
90°	55°	$\sim 50°$
$110 \rightarrow 160°$	no soln	unstable
170°	156°	$\sim 150°$
180°	180°	$\sim 180°$

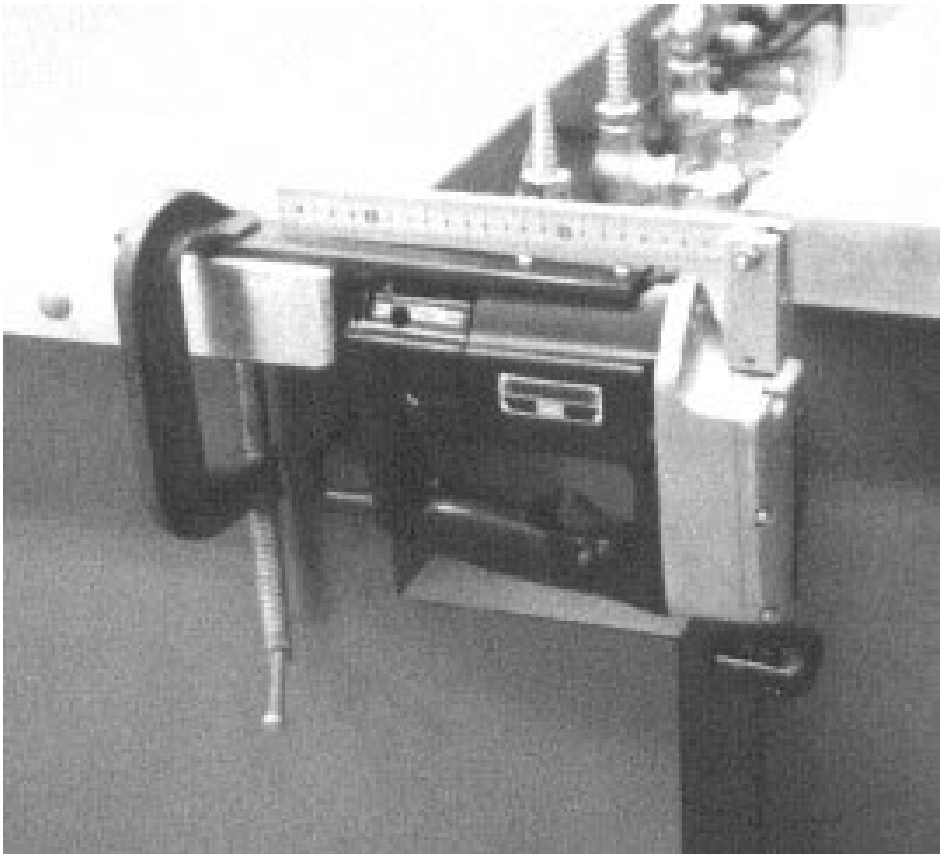

FIG. 1: The UC Riverside Driven Pendulum

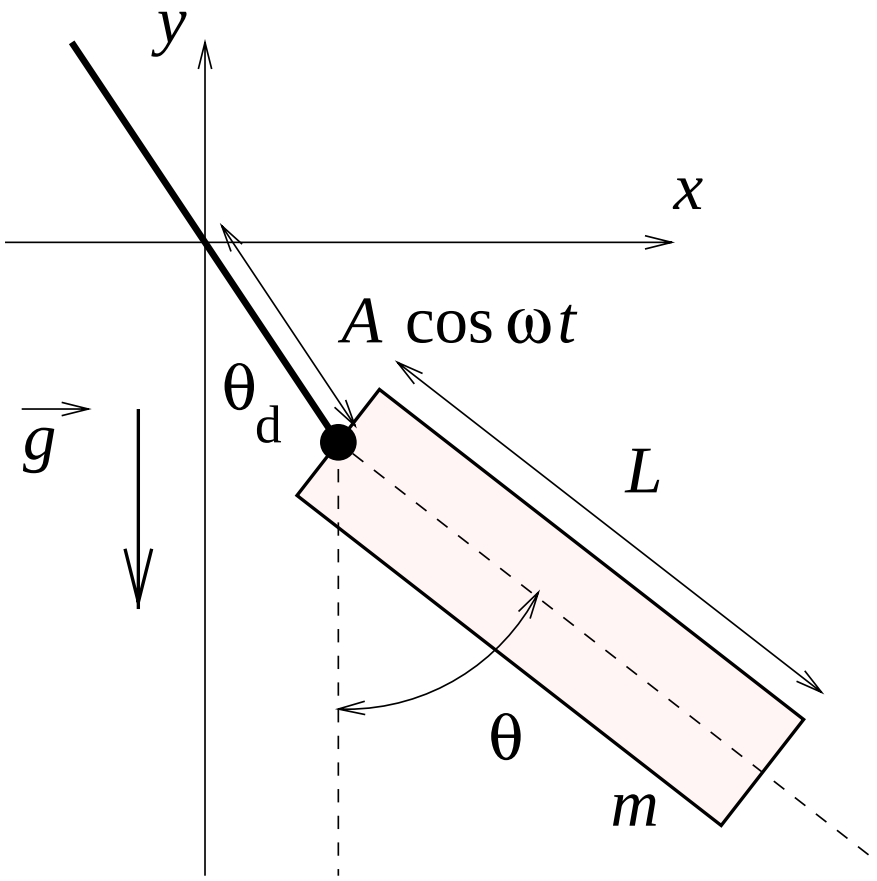

FIG. 2: The Pendulum Driven at Angle $\theta_{\rm d}$

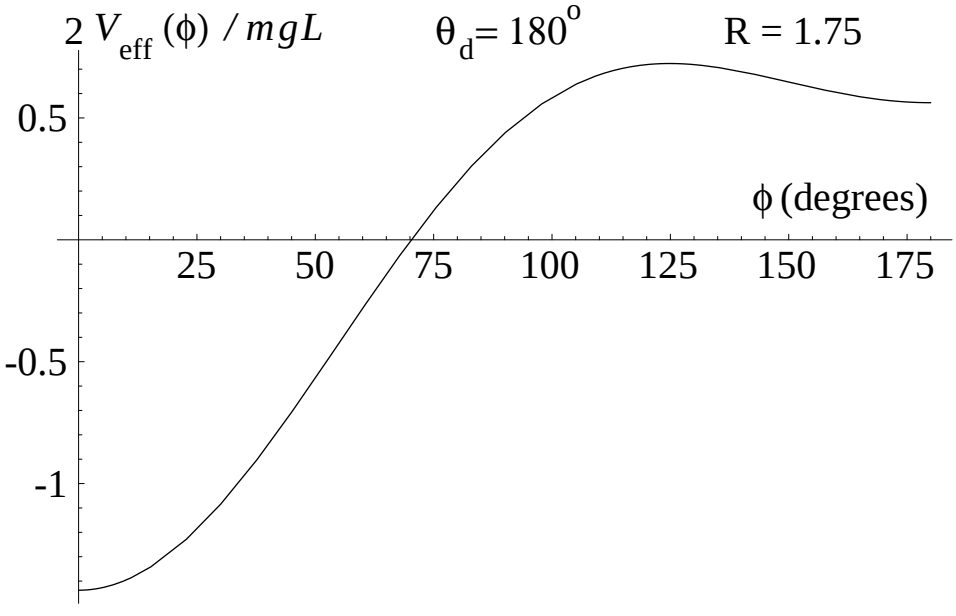

FIG. 3: $V_{\rm eff}(\phi)$ for an driven inverted pendulum ($\theta_{\rm d} = 180°$)

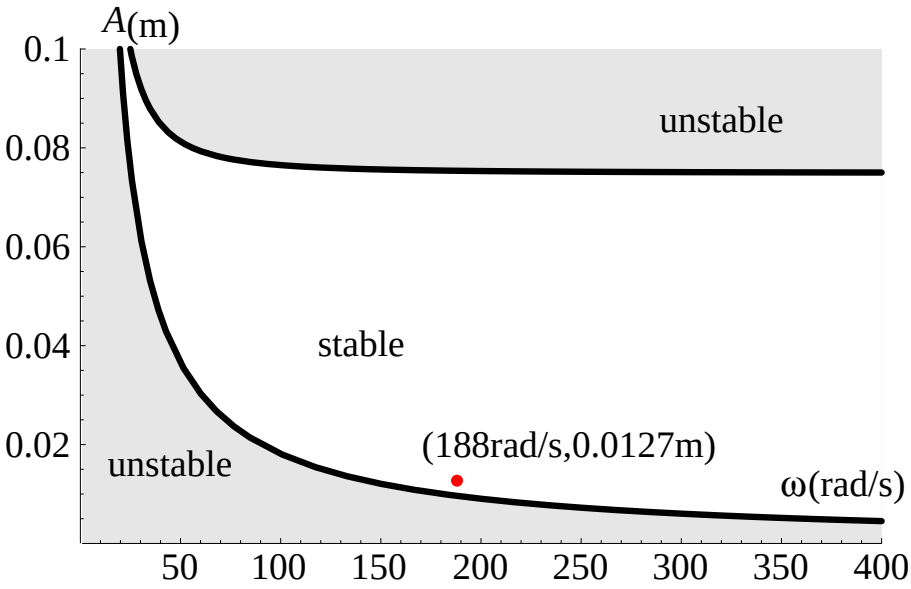

FIG. 4: The stable region in drive amplitude A and angular frequency ω for a driven inverted pendulum of length $L = 0.25$m. The parameters of the UC Riverside pendulum are shown as a point at $A = 0.0127$m and $\omega = 188/$s.

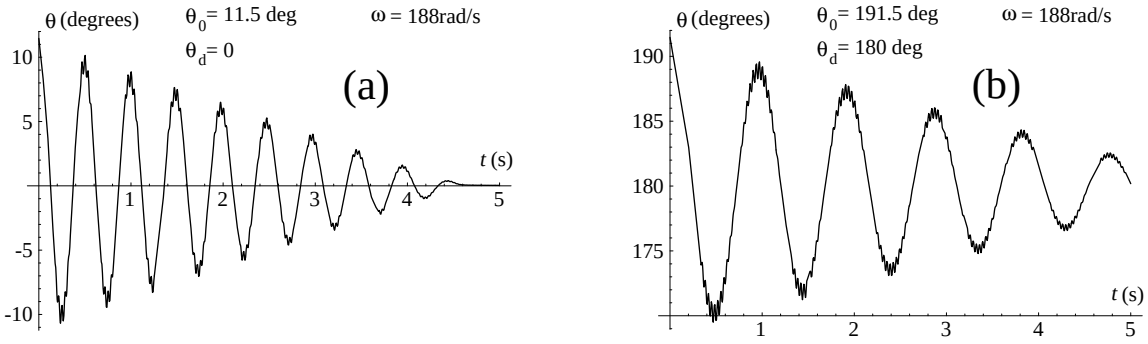

FIG. 5: Motion for (a) $\theta_{\rm d} = 0$, and (b) $\theta_{\rm d} = 180°$, with ad hoc frictional damping (described in Appendix B)

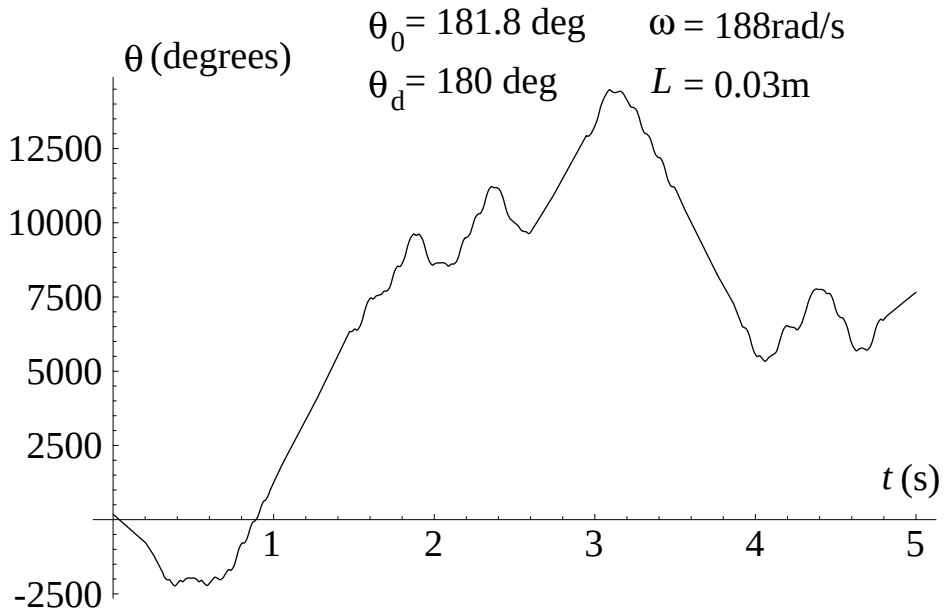

FIG. 6: Over-driven inverted pendulum, of the type modeled in Fig. 5, with rod length 3cm ($L = 0.03$m). No stable solution is found or observed.

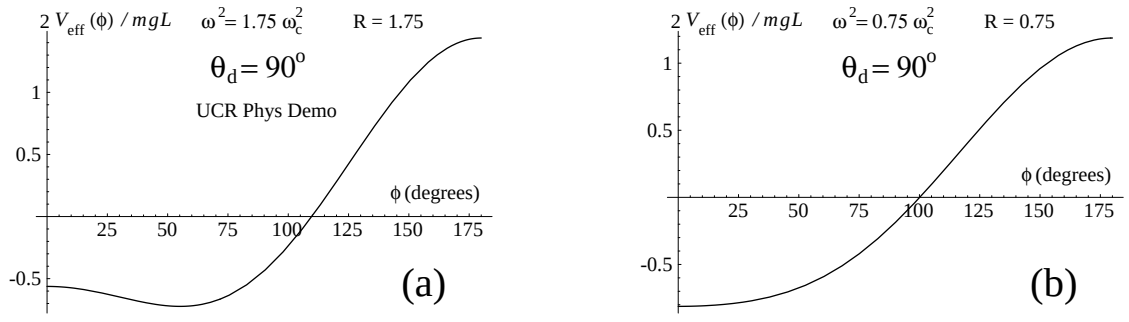

FIG. 7: (a) for $R = \omega^2/\omega_c^2 = 1.75$ there is a minimum at $\phi_0 \simeq 55°$, while the equilibrium at 0 degrees becomes *unstable*. (b) for $\omega < \omega_c$ the only minimum in $V_{\rm eff}(\phi)$ is at $\phi_0 = 0$.

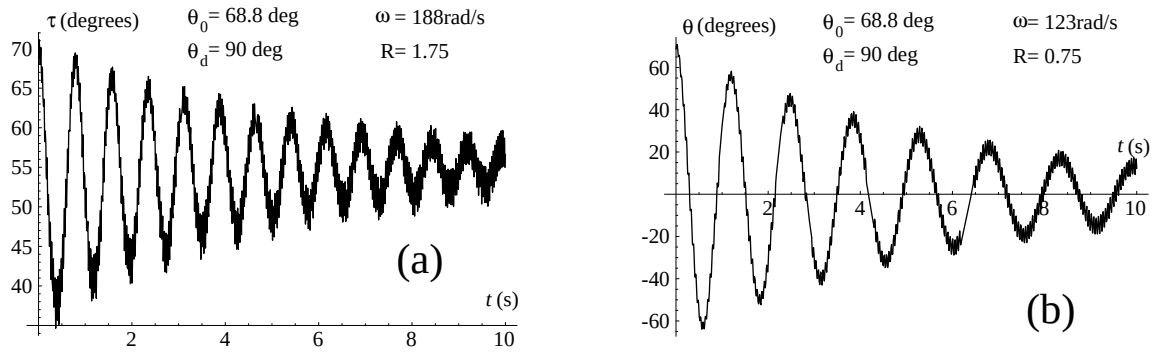

FIG. 8: Motion for $\theta_{\rm d} = 90°$ with (a) $R = 1.75$ (stable about 55°), and (b) $R = 0.75$ (stable about 0°). This matches well to the predictions in Figs. 7(a) and (b).

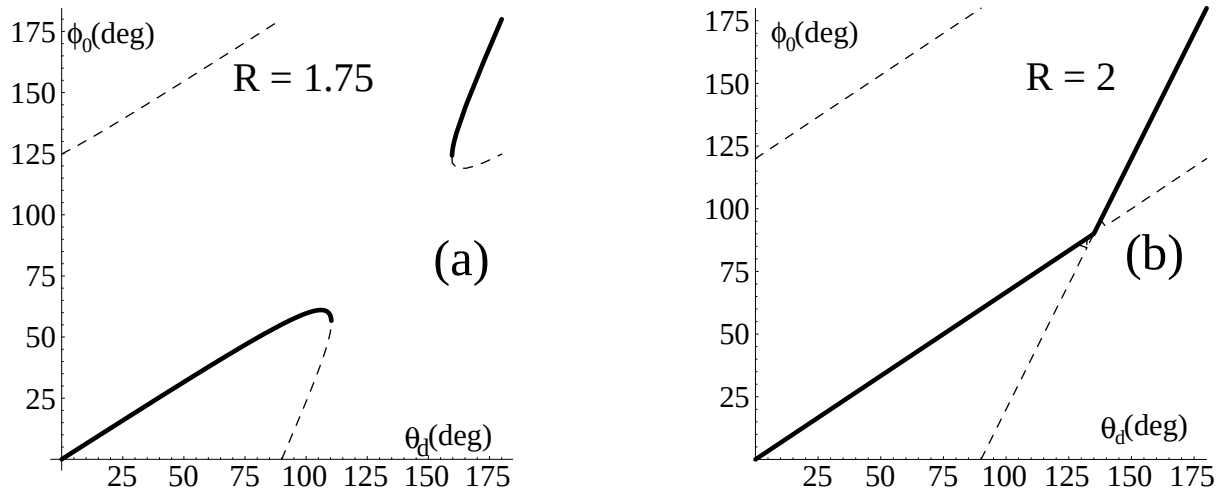

FIG. 9: All equilibriums (dashed) and *stable* equilibriums (solid line) in ϕ_0 vs. $\theta_{\rm d}$ for (a) $R = 1.75$, and (b) $R = 2$.

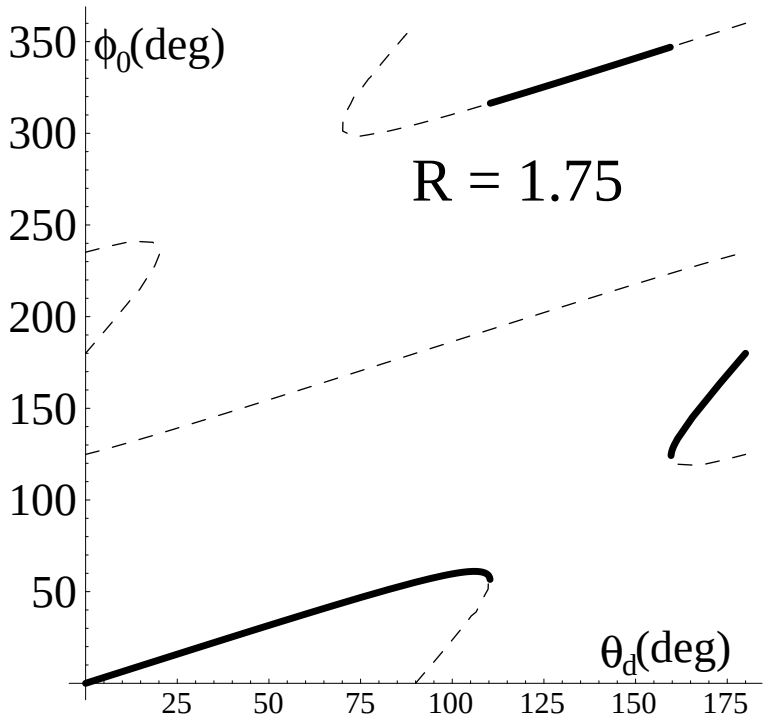

FIG. 10: ϕ_0 vs. θ_d for $R = 1.75$, including solutions at $\phi_0 > 180°$.

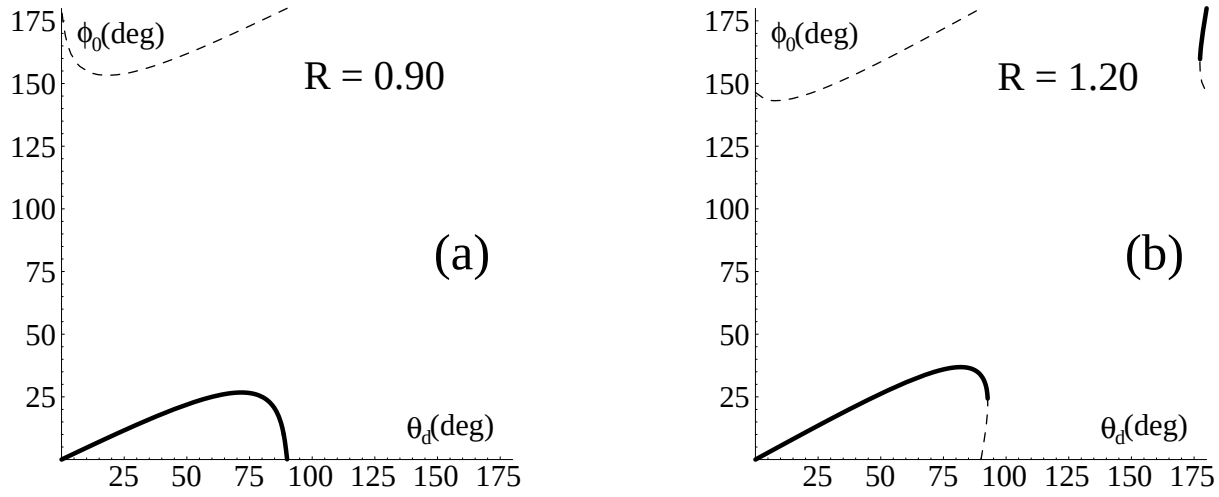

FIG. 11: All equilibriums (dashed) and *stable* equilibriums (solid) in ϕ_0 vs. θ_d for (a) $R = 0.90$, and (b) $R = 1.20$.

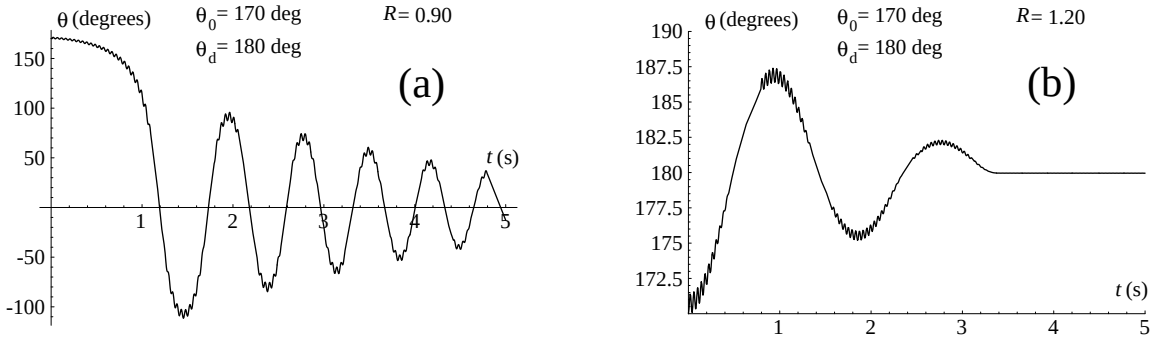

FIG. 12: Motion for $\theta_{\rm d} = 180°$ and $\theta_0 = 170°$, with (a) $R = 0.90$, and (b) $R = 1.20$.

FIG. 13: The Embry-Riddle Aeronautical University driven pendulum

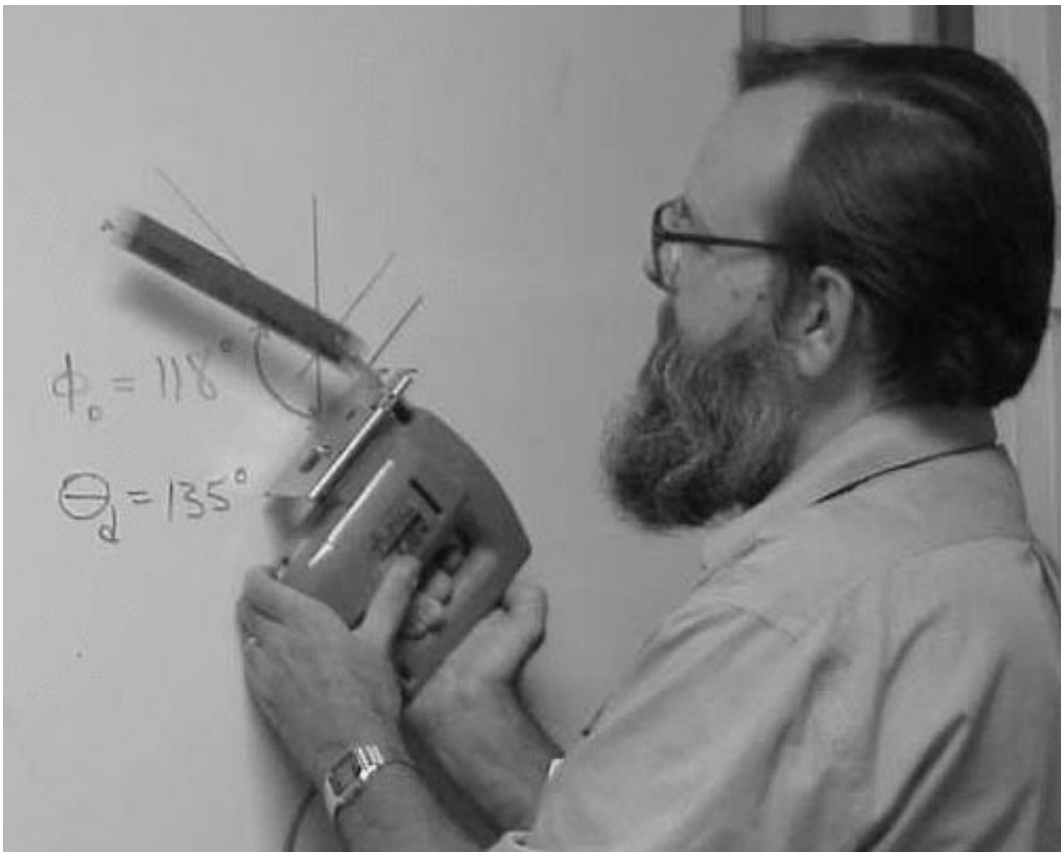

FIG. 14: The ERAU driven pendulum with $R = 3.2$ and $\theta_d = 135°$ displaying stability at $\phi_0 \simeq 118°$

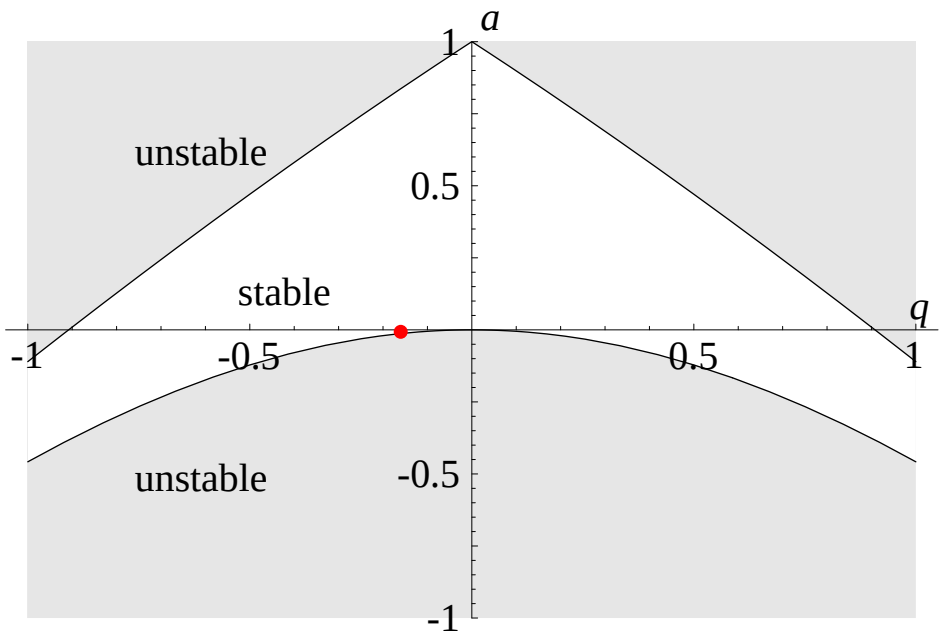

FIG. 15: The stable region in the Mathieu parameters a and q for a driven inverted pendulum. The parameters of the UC Riverside pendulum are shown as a point at $q = -0.00665$ and $a = -0.1524$.

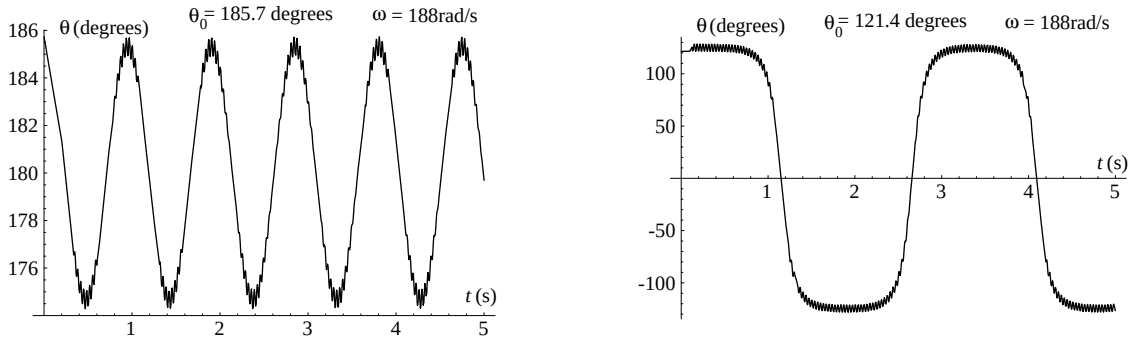

FIG. 16: Numerical solution of the driven inverted pendulum: (a) small starting deviation ($\theta_0 = 185.7°$), and (b) large starting deviation ($\theta_0 = 121.4°$)

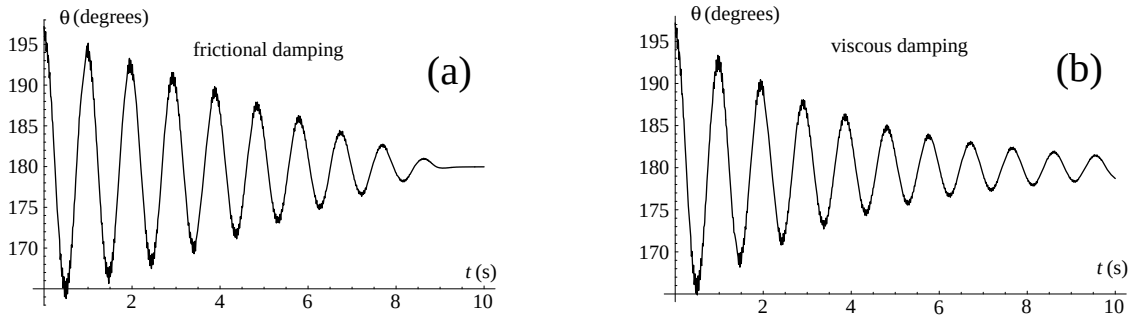

FIG. 17: Simulation of the driven inverted pendulum including (a) frictional damping, and (b) viscous damping.